2021 43rd Annual International Conference of the
IEEE Engineering in Medicine & Biology Society (EMBC)
Oct 31 - Nov 4, 2021. Virtual Conference

Dynamic patterns within the default mode network in schizophrenia subgroups

Mohammad S. E. Sendi *Student Member, IEEE*, Elaheh Zendehrouh, Jessica A. Turner Vince D. Calhoun, *Fellow, IEEE*

Abstract— **In this study, resting-state functional magnetic resonance imaging (rs-fMRI) data of 125 schizophrenia (SZ) subjects were analyzed. Based on SZ demographic information and cognitive scores and using an unsupervised clustering method, we identified subgroups of patients and compared DMN dynamic functional connectivity (dFC) between the groups. We captured seven independent subnodes, including anterior cingulate cortex (ACC), posterior cingulate cortex (PCC), and precuneus (PCu), in the DMN by applying group independent component analysis (group-ICA) and estimated dFC between component time courses using a sliding window approach. By using k-means clustering, we separated the dFCs into three reoccurring brain states. Using the statistical method, we compared the state-specific DMN connectivity pattern between two SZ subgroups. In addition, we used a transition probability matrix of a hidden Markov model (HMM) and occupancy rate (OCR) of each state between two SZ subgroups. We found SZ subjects with higher positive and negative syndrome scale (PNASS) showed lower within ACC and lower ACC and PCC connectivity (or ACC/PCC). In addition, we found the transition from state1 to same state is significantly different between two groups, while this result was not significant after multiple comparison tests**.

I. Introduction

Schizophrenia (SZ) affects around 1% of the whole adult population [1], which exhibits widespread dysconnectivity. In recent years, functional connectivity (FC) obtained from resting-state functional magnetic resonance imaging (rs-fMRI) time series has revealed a great deal of knowledge about these brain dysconnectivity in schizophrenia [2]. More recently, work has focused on the dynamics of FC or dFC [3], [4]. However, most of these studies focus only on comparing the FC of healthy control (HC) and SZ subject, and less work has been done on different subgroups of SZ subjects.

Among brain networks, the default mode network (DMN) - including anterior cingulate cortex (ACC), posterior cingulate cortex (PCC), precuneus (PCu), medial prefrontal cortex (mPFC), and lateral and inferior parietal cortex, has been the most widely studied due to its putative role in the underlying external monitoring, spontaneous cognition, and autobiographical thinking [5] and linked to mental disorders including schizophrenia. In this paper, to investigate the temporal dynamics of FC within DMN in two subgroups of SZ subject. We extracted seven data-driven subnodes within DMN. Then, we used a sliding window approach, and later k-means clustering the dFC to identify a set of connectivity states [6]. Next, to investigate the temporal changes in dFC, we estimated the transition probability of the hidden Markov model (HMM) and occupancy rate (OCR) features from dFC. Finally, via statistical analysis on the estimated features, we compared two subgroups of SZ subjects.

II. Materials and Methods

A. Participants

In this study, the resting-state fMRI and clinical data of 125 SZ subjects were from the Functional Imaging Biomedical Informatics Research Network (FBIRN) projects [7]. The raw imaging data were collected from seven sites including the University of California, Irvine; the University of California, Los Angeles; the University of California, San Francisco; Duke University/the University of North Carolina at Chapel Hill; the University of New Mexico; the University of Iowa; and the University of Minnesota. The written informed consent, approved by institutional review boards of each study site, was obtained from all subjects. T2*-weighted functional images were collected using AC-PC aligned echo-planar imaging sequence with TE=30ms, TR=2s, flip angle = 77°, slice gap=1 mm, voxel size= 3.4 × 3.4 × 4 mm^3, and 162

M. S. E. Sendi (msendi6@gatech.edu), and V. D. Calhoun (vcalhoun@gsu.edu) are with the Department of Electrical and Computer Engineering at Georgia Institute of Technology, Atlanta, Georgia, Wallace H. Coulter Department of Biomedical Engineering at Georgia Institute of Technology and Emory University, Atlanta, Georgia.

M. S. E. Sendi, J. A. Turner (jturner63@gsu.edu), and V. D. Calhoun are with Tri-institutional Center for Translational Research in Neuroimaging and Data Science: Georgia State University, Georgia Institute of Technology, Emory University Atlanta, Georgia.

E. Zendehrouh (ezendehrouh1@student.gsu.edu), J.A. Turner, and V. D. Calhoun are with Georgia State University, Atlanta, Georgia. J. A. Turner is with Department of Psychology, Georgia State University, Atlanta, Georgia, and with Neuroscience Institute, Georgia State University, Atlanta, Georgia.

This work was supported by National Institute of Health under R01EB006841 R01EB020407, R01MH121246, R01MH117107, and R01MH118695.

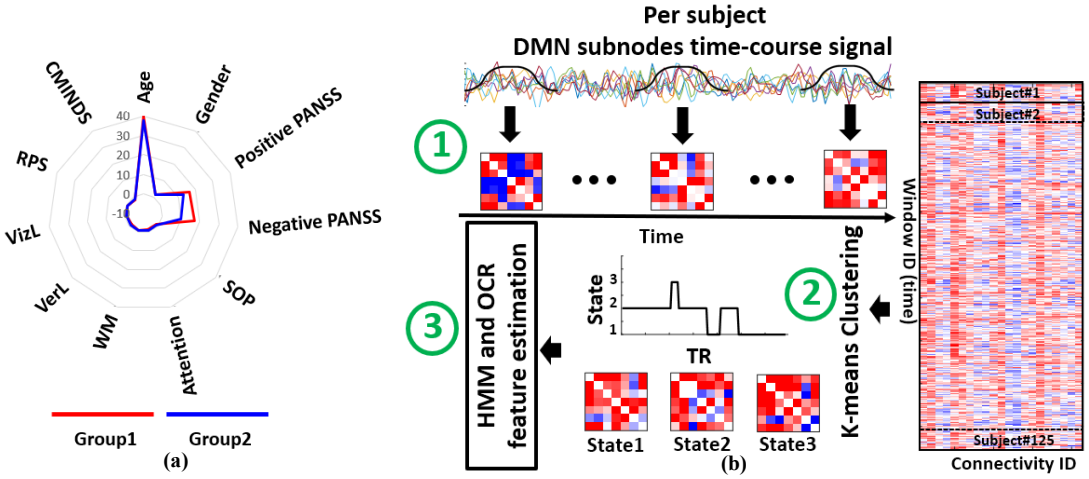

Fig.1. a) Two subgroups of schizophrenia subjects identified by clustering method based on their clinical information. b) Analytic pipeline used in this study: Step1: The time-course signal of seven subnodes in default mode network (DMN) has been identified using Neuromark. After identifying seven subnodes in DMN, a taper sliding window was used to segment the time-course signals and then calculated the functional connectivity (FC) matrix. Each FC matrix contains twenty-one connectivity features. Step2: We have concatenated them and then a k-means clustering with was used to group FCs to five distinct clusters. Step3: Then, hidden Markov model (HMM), in total nine features, and occupancy rate (OCR), in total three features, were calculated from the state vector of each subject. We investigated the difference between two subgroups of SZ subjects based on HMM and OCR and state-specific connectivity features. PANSS: Positive and negative syndrome scale, SOP: Speed of processing , WM: Working memory, VerL: Verbal learning, VizL: Visual learning. RPS: Reasoning problem solving, CMINDS Comp: Computerized multiphasic interactive neurocognitive system CMINDS composite.

frames, and 5:24 (min:sec). All participants were instructed to close their eyes during the rs-fMRI data collection.

The demographic data and cognitive scores included age, gender, positive and negative syndrome scale or PANSS (P), PANSS (N), speed of processing (SOP), attention, working memory (WM), verbal learning (VerL), visual learning (VizL), reasoning problem solving (RPS), and computerized multiphasic interactive neurocognitive system or CMINDS_composite. The detail of the cognitive score collection is provided in [7]. An unsupervised clustering method was used to put the SZ subjects into two groups based on these data. Group 1 and Group 2 included 69 and 56 subjects. Fig.1a compares these two groups.

B. Data Acquisition

Two scanners of TIM Trio 3T (Siemens Medical Solutions USA, Inc) with a 20 channel head coil on 3T scanners were used to collect rs-fMRI. High resolution T2*-weighted functional images were acquired using echoplanar imaging or EP sequence with TE =27 ms, TR = 2.2 s, flip angle = 90˚, slice thickness = 4mm, slice gap (center-to-center) = 4 mm, matrix size = 64, and field of view (FOV)= 256×256×128 mm3. The duration of the scanning was 6 minutes.

C. Preprocessing

We preprocessed the fMRI data in the statistical parametric mapping (SPM12, http://www.fil.ion.ucl.ac.uk/spm/). We used the Neuromark pipeline to extract reliable intrinsic connectivity networks (ICNs) within GIFT (http://trendscenter.org/software/gift) [8]. NeuroMark is a fully automated independent component analysis (ICA) framework that uses spatially constrained ICA to estimate comparable features across subjects by taking advantage of the replicated brain network templates extracted from two N~900 normative resting fMRI data sets. ICNs were grouped into seven domains based on anatomy and prior knowledge of their function. Using this template, we extracted seven components (subnodes) within DMN. These seven subnodes included three precunei (PCu), two anterior cingulate cortex (ACC), and two posterior cingulate cortex (PCC) [8]. Table 2 shows these seven subnodes within DMN.

D. Dynamic functional connectivity estimation

For each subject $i = 1 \ldots N$, we estimated the dFC via a sliding window approach. To localize the dataset at each time point, we used a tapered window, which was obtained by convolving a rectangle (window size = 20 TRs = 40 s) with a Gaussian (σ = 3). Then, we calculated the covariance matrix for each window data to measure the dFC between ICNs. Next, we concatenated dFC estimates of each window for each subject to form a $C \times C \times T$ array (where $C=7$ denotes the number of subnodes within DMN and T=137 denotes the number of windows), which represented the changes in brain connectivity between ICNs as a function of time [3]. This process shows in Step 1 in Fig. 1.

E. Clustering and temporal modeling

After calculating the dFC of each subject in both groups, we combined them, as shown in Step 2 of Fig.1. Then, we used a *k*-means algorithm, where k=3, to these dFC windows to partition the data into a set of separated clusters. We estimated the optimal number of centroid states using the elbow criterion based on the ratio of within to between cluster distance. In a search window of *k* from 2 to 9, we found that the optimal

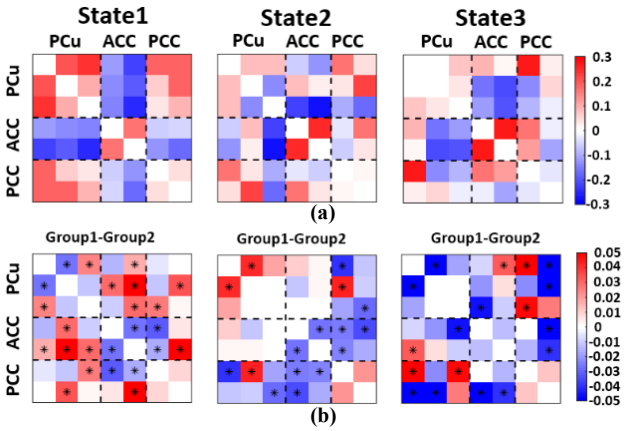

Fig.2. a) Three states identified by k-means clustering method based on seven subnodes within DMN. The color bar shows the strength of the connectivity, where the blue shows negative and red shows positive connectivity. b) The DMN dFC difference between Group1 and Group2 subjects (Group1-Group2) in each state. Significant group differences passing the multiple comparison threshold are marked by asterisks (false discovery rate [FDR] corrected, q = 0.05). PCu: Precuneus, ACC: Anterior cingulate cortex, PCC: Posterior cingulate cortex.

number of clusters is 3. we used correlation as a distance metric. This step resulted in 3 matrices; each showed the center of each cluster and state vector of each subject, as shown in Fig.1b.

Next, for each subject, we calculated the transition probability between states via HMM, and this probability was used as a latent feature of dFC. The transition probability, a_{ij}, is the probability of the system to transition from state j at time t to state i at time $t+1$. (Step3 in Figure 1). For each subject, nine HMM features were obtained from three states. Also, using state vector, we found the portion of time each subject spent in each state. We called this feature the occupancy rate (OCR) of each state. In total, we had three OCRs for each subject.

F. Statistical Analysis

We compared the HMM, OCR, and the DMN connectivity features between two groups using a two-sample t-test. In all statistics, p values were adjusted by the Benjamini-Hochberg correction method for multiple comparisons [9].

III. Results

A. Demographic and clinical difference between Group1 and Group2

We compared the clinical and demographic information between two groups using a two-sample t-test. Among all clinical information, we found a significant difference in positive and negative PANSS between the two groups. As shown in Fig. 1a, Group 1 showed higher positive and negative PANSS compared with those of Group 2 (corrected $p<0.001$). For Group1, the average of positive and negative PANSS was 16.5507 and 17.2754, respectively. In Group 2, the average positive and negative PANSS were 13.0357 and 9.8036, respectively. Other clinical and demographic scores did not show any significant difference between the two groups.

B. Dynamic functional connectivity states

Fig. 2a shows the three reoccurring dFC states identified by *k*-means clustering. As shown in Fig.2a, we see different connectivity patterns in different states. In state 1, we observed positive connectivity within PCu, within ACC, and within PCC subnodes. This state was separated from other states by showing negative connectivity between ACC subnodes and other subnodes of DMN. This state was the only one that showed only positive connectivity between PCus and PCCs. State 2 showed both positive and negative connectivity within PCu subnodes. In this state, within ACC connectivity was positive. The connectivity between PCu and ACC, between PCu and PCC, and between ACC and PCC showed both positive and negative connectivity. In state 3, within PCu connectivity, and within ACC, connectivity was positive. While within PCC, connectivity was negative. Similar to state2, this state showed both positive and negative pattern in the connectivity between PCu and ACC, between PCu and PCC, and between ACC and PCC.

C. Regional connectivity differences between Group1 and Group2 connectivity in each state

To test for the DMN connectivity differences between Group1 subjects and Group2 subjects in each state, we used two-sample t-tests. The results are shown in Fig. 2b. Significant group differences passing the multiple comparison testing are marked by asterisks (false discovery rate [FDR] corrected, q = 0.05). Interestingly, all states showed significant differences between the two groups. In all three states, we observed a disrupted pattern in DMN connectivity. Overall, Group1 with higher positive and negative PANSS showed more DMN connectivity is state 1 and less DMN connectivity in state 2 and state 3 than that of Group2. In all state, within-ACC connectivity is significantly lower in Group1, while the difference between Group1 and Group2 is not significant after FDR correction in state 3. Within PCu connectivity of Group1 is higher in state2 and lower in state 3. Within PCC connectivity was higher in all states and but did not survived multiple comparison tests. The connectivity between ACC and PCC (ACC/PCC) was lower for Group1 in state 2 and state 3.

D. Temporal differences between Group1 and Group2

In the next step, we compare the OCR of each state between Group 1 and Group 2. We did not find any significant difference between Group 1 and Group 2 based on their OCR of each state. Finally, we compared the HMM features between Group 1 and Group 2. Only the transition from state1 to state 1, i.e., a_{11}, showed a significant difference between two groups (uncorrected $p=0.04$). But this difference was not significant after multiple comparisons.

IV. Discussion

For the first time, we explored the DMN, including PCu, ACC, and PCC, connectivity difference between two groups of SZ subjects, which showed a significant difference between their symptom severity. We found a lower ACC

connectivity of subgroup with higher positive and negative symptom severity. A recent study found a lower ACC connectivity for SZ subjects compared to healthy control (HC)[10]. Our new finding suggested that ACC connectivity might be lower in SZ subjects with higher symptom severity. Also, we found higher PCC connectivity for the subjects with higher symptom severity. However, this difference was not significant after multiple comparisons. This finding is consistent with the previous study, which showed SZ subject had higher PCC connectivity compared with that of HC subjects[11].

In all states, we found a disrupted pattern within PCu connectivity by showing both higher and lower connectivity in subjects with higher symptom severity compared with those subjects with lower symptom severity. In state 1, we found higher PCu/PCC connectivity in Group1, while this connectivity was both higher and lower for Group 1 in state 2 and state 3. Previous studies reported both increase and decrease in PCu/PCC connectivity [12], [13]·[14] in the connectivity between PCu and PCC in SZ subjects compared with HC ones. These inconsistent results possibly could be focusing on static FC and averaging of the functional connectivity across time. Here, which showed a disrupted pattern of PCu/PCC connectivity, potentially highlighted the importance of the study of functional connectivity in a shorter time. In addition, we found lower ACC/PCC connectivity for Group 1 in two states. That means that the ACC/PCC connectivity is lower with SZ subject with higher positive and negative PANSS. This result is consistent with the result of the previous study, which showed SZ subjects with higher positive symptom score of PANSS has lower ACC/PCC connectivity [15].

V. Conclusion

In this paper, we investigated differences in the connectivity of data driven DMN subnodes of two different groups of schizophrenia subjects. Results showed a highly dynamic pattern within DMN. Schizophrenia subjects with higher positive PANSS showed lower ACC, higher PCC, and lower ACC/PCC connectivity. Also, we found a disrupted PCu/PCC connectivity in this network.

VI. References

[1] R. S. Kahn *et al.*, "Schizophrenia," *Nature Reviews Disease Primers*, vol. 1, no. November, 2015.

[2] M. E. Lynall *et al.*, "Functional connectivity and brain networks in schizophrenia," *Journal of Neuroscience*, vol. 30, no. 28, pp. 9477–9487, 2010.

[3] S. Bhinge, Q. Long, V. D. Calhoun, and T. Adali, "Spatial Dynamic Functional Connectivity Analysis Identifies Distinctive Biomarkers in Schizophrenia," *Frontiers in Neuroscience*, vol. 13, no. September, 2019.

[4] E. Damaraju *et al.*, "Dynamic functional connectivity analysis reveals transient states of dysconnectivity in schizophrenia," *NeuroImage: Clinical*, vol. 5, no. July, pp. 298–308, 2014.

[5] M. L. Hu *et al.*, "A Review of the Functional and Anatomical Default Mode Network in Schizophrenia," *Neuroscience Bulletin*, vol. 33, no. 1, pp. 73–84, 2017.

[6] M. S. E. Sendi, E. Zendehrouh, Z. Fu, B. Mahmoudi, R. L. Miller, and V. D. Calhoun, "A Machine Learning Model for Exploring Aberrant Functional Network Connectivity Transition in Schizophrenia," in *IEEE Southwest Symposium on IEEE Southwest Symposium on*, 2020, pp. 112–115.

[7] T. G. M. Van Erp *et al.*, "Neuropsychological profile in adult schizophrenia measured with the CMINDS," *Psychiatry Research*, vol. 230, no. 3, pp. 826–834, 2015.

[8] Y. Du *et al.*, "NeuroMark: An automated and adaptive ICA based pipeline to identify reproducible fMRI markers of brain disorders," *NeuroImage: Clinical*, vol. 28, no. August, p. 102375, 2020.

[9] Yoav Benjamini ; Yosef Hochberg, "Controlling the False Discovery Rate : A Practical and Powerful Approach to Multiple Testing," *Royal Statistical Society . Series B (Methodological)*, vol. 57, no. 1, pp. 289–300, 1995.

[10] D. K. Shukla *et al.*, "Anterior cingulate glutamate and GABA associations on functional connectivity in schizophrenia," *Schizophrenia Bulletin*, vol. 45, no. 3, pp. 647–658, 2019.

[11] S. Whitfield-Gabrieli *et al.*, "Hyperactivity and hyperconnectivity of the default network in schizophrenia and in first-degree relatives of persons with schizophrenia," *Proceedings of the National Academy of Sciences of the United States of America*, vol. 106, no. 4, pp. 1279–1284, 2009.

[12] S. C. T. Peeters *et al.*, "Default mode network connectivity as a function of familial and environmental risk for psychotic disorder," *PLoS ONE*, vol. 10, no. 3, pp. 1–19, 2015.

[13] S. Whitfield-Gabrieli *et al.*, "Hyperactivity and hyperconnectivity of the default network in schizophrenia and in first-degree relatives of persons with schizophrenia," *Proceedings of the National Academy of Sciences of the United States of America*, vol. 106, no. 4, pp. 1279–1284, 2009.

[14] X. Wang *et al.*, "Disrupted resting-state functional connectivity in minimally treated chronic schizophrenia," *Schizophrenia Research*, vol. 156, no. 2–3, pp. 150–156, 2014.

[15] H. Yan *et al.*, "Functional and Anatomical Connectivity Abnormalities in Cognitive Division of Anterior Cingulate Cortex in Schizophrenia," *PLoS ONE*, vol. 7, no. 9, 2012.